# DETECTION OF THE TEA LEAVES WILTING LEVEL WITH DLSI (DYNAMIC SPECKLE LASER IMAGING) NUMERICAL ANALYSIS

**Wiwis Sasmitaninghidayah[1], Dian Rahmawati[1], Ainatul Mardhiyah[2], Naqiibatin Nadliriyah[1], Imam Tazi[1]**

*[1]Department of Physics, Faculty of Science and Technology, Universitas Islam Negeri Maulana Malik Ibrahim Malang, Indonesia*
*[2]Department of Basic Education Science and Islam, Faculty of Islamic Education and Teaching Sciences, Universitas Islam Negeri Maulana Malik Ibrahim Malang, Indonesia*

***Received:6th September 2024 ; Revised: 20th March 2025; Accepted: 20th March 2025***

**ABSTRACT**

This study aimed to find a correlation between the degree of tealight and the speckle image of the tea leaf by using numerical analysis and graphical analysis. Numerical analysis was done using THSP (*Time History Of Speckle Patterns*), COM (*Co-occurrence Matrix*), IM (*Inertia Moment)*, and AVD (*Average Value of Difference*) values. The numbers used in the study showed that THSP and correlation measurements showed changes in the biological activity of tea leaves at all wilting levels. Meanwhile, the IM and AVD values showed significant changes after the tea leaves withered by 57.56%. COM analysis did not show any changes from high to low levels. THSP and correlation measurement showed changes in biological activity in tea leaves. Biological activity was high at high water content, and biological activity decreased as the water content in tea leaves decreased.

**Keywords:** DSLI; THSP; Speckel; Wilting Tea Level;

## Introduction

Tea was one of the most widely consumed beverages globally. Tea was unique because a wide variety of secondary metabolites were present in its leaves.[1] including soluble sugars, amino acids, phenolic compounds, and aroma compounds (volatiles). Each of these components provided different organoleptic characteristics (such as taste, color, and aroma) and health-related properties.[2] Various types of tea were produced from processing shoots with 2-3 young leaves (P+2 or P+3). In principle, the tea processing process was divided into three types: tea without oxidation (white tea, green tea), semi-oxidized tea (oolong tea), and tea with an oxidation process (black tea).[3]

Pre- and post-harvest conditions effectively influenced tea quality. Exposure to cold, dryness, light, or insects at pre-harvest improved the tea's flavor, whereas wounding, drying, or low temperatures applied at post-harvest enhanced the tea's aroma.[2] Several previous methods of drying herbal tea used the room-temperature drying method, where tea was consumed directly by boiling soursat leaves, fragrant pandan leaves, and quinine manga leaves in the oven at a temperature of 50°C and drying the fig leaves in a cabinet dryer at a temperature of 55°C–65°C for 4–6 hours.[4] All drying methods required effective control so that the tea had the desired quality.

Biospeckle laser (BSL) was a sensitive interferometric phenomenon for monitoring subtle changes in biological samples and had been adopted as a tool that could be applied in many fields, from medicine to agriculture. Its main advantages were related to the simplicity of the required apparatus as well as to its being a relevant non-destructive test (NDT) in biological applications. The multitude of applications demanded the emergence of methods for illuminating, assembling images,

*Corresponding author.
E-Mail: wiwis_hidayah_87@fis.uin-malang.ac.id

and providing analysis. Dynamic laser speckle analysis as a source of information about the activity of biological or even non-biological materials requires a lot of image processing-related mathematical and statistical approaches.[5]

Laser speckle imaging (LSI) is recognized as a powerful and noninvasive measurement tool with diverse applications in biomedical and agricultural research. In medicine, LSI enables real-time monitoring of blood flow dynamics and provides important insights into vascular function,[6] and is also useful in neurosurgery, facilitating intraoperative visualization of cerebral blood flow with high spatiotemporal resolution.[7,8] Furthermore, LSI has been adapted for ophthalmology, enabling portable and noninvasive imaging of retinal blood flow.[9] LSI has shown promising results in dermatology for predicting skin conditions[10] and in agriculture for the early detection of fungal infections in plants.[11] The technique's versatility, real-time capabilities, and noninvasive nature make it a valuable imaging modality in a variety of scientific and medical fields.[12]

The laser speckle technique was based on the diffusion of light with a diffusing medium. The medium of distribution of each cell or active sample contained various types of randomly moving particles (scatter). When a laser beam attacked a sample, light diffused through the sample medium and formed a random interference pattern called a laser speckle. The intensity at a certain point of the speckle changed rapidly due to the dynamics of the spread, and this was called laser speckle dynamics. It was a non-invasive, non-destructive, and innovative technique that provided information about activity in sample media and behavior. Changes in the pixel value at a particular position in the speckled image were related to the speckling activity of the sample. The time history of speckle patterns (THSP), COM (matrix co-occurrence), IM, and AVD correlation provided qualitative information about activity. THSP was constructed by selecting one row or column from each image from all the recorded speckle images. Each row and column was not identical for the whole image. Thus, THSP did not have a unique shape for the entire recorded sample area. COM was defined on one image, and one speckle image did not convey much of the dynamic behavior of the sample. So, for the analysis of dynamic laser speckles, COM was defined through THSP images. The selection of numerical methods for speckle image analysis was because the sample used was a homogeneous sample.[5]

## Methods

The toolset used was the backscattering tool set.

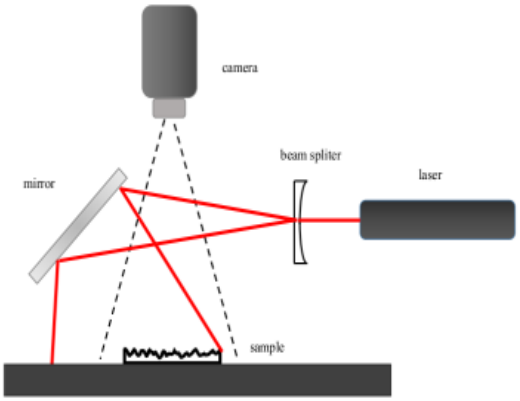


**Figure 1.** Backscattering tool set[5]

The water content of tea was analyzed using the equation:

$$\ldots\% = \frac{final\ weight - initial\ weight}{initial\ weight}\ x\ 100\%$$

(13).

The reduction in water content was obtained by heating the tea leaves at a temperature of 70 ºC. Speckle Data Specifications Results of Data Collection with a Digital Microscope Format: PNG, JPG Image size: 640 x 480 pixels Color: Gray Scale Processing Results Format: BMP Image size: 448 x 448 pixels Color: 8-bit color. The correlation of wilting and speckle images on tea leaves was obtained by carrying out numerical analysis in the form of THSP, COM, and correlation

## Result and Discussion

The THSP pattern was a matrix with only one column or line represented in the S position of all Ik matrices, while the other columns or lines were discarded. The THSP pattern of tea leaves with a water content of 100% and 27.72% was shown in Figure 2 below.

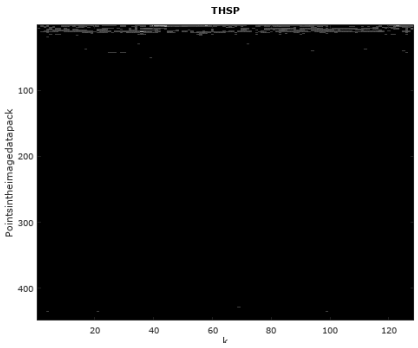


a.

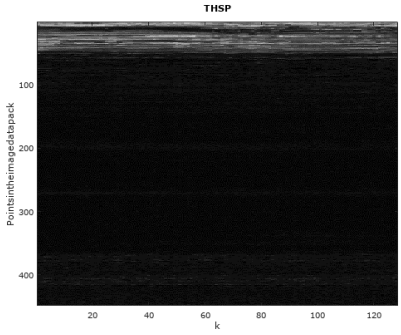


b.

**Figure 2.** THSP pattern formed from tea water content, a. 100%, b. 27.72 %

Figure 2 shows the difference in the THSP pattern, which means that there is a difference in tea leaf cell activity in the two conditions. At 100% water content, high biological activity was indicated by the tightness of the THSP pattern lines formed. Along with the decrease in water levels, there was a decline in concentration. Some of the lines turned white, indicating that there was a decrease in cell activity in the tea leaf. This was in line with the fact that in fresh tea leaves, intercellular activity was still high, but along with drying, resulting in decreased water content, intercellular activity within the leaf also decreased.

The Co-occurrence Matrix (COM) was an intermediate matrix used to evaluate the sequential pixel dispersion in the THSP monitoring point M through N samples, as shown in Equation (2),

$$COM(i,j)=\sum_{m=1}^{M}\sum_{n=1}^{N-1}\begin{cases}1, & \text{if } THSP(m,n)=i \text{ and } THSP(m,n+1)=j\\ 0, & \text{otherwise}\end{cases} \quad (2)$$

where the COM matrix represented the intensity transition histogram. Thus, COM (i, j) had a transition as to how many times the intensity level I to J occurred.

The co-occurrence of the matrix of the THSP model formed by the tea image was presented as follows:

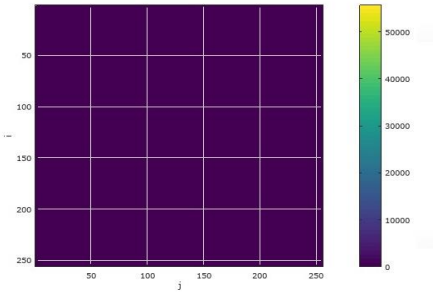


a.

b.

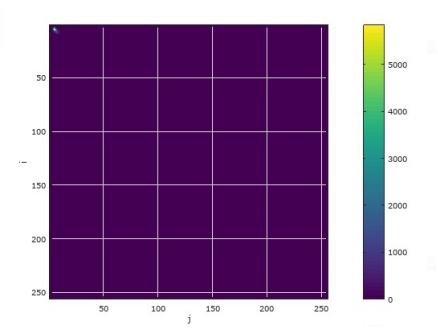


**Figure 3.** Co-occurance Matrix of the THSP tea leaf image at the time of the water level of a. 100%, b. 27.22%

Showed there was a small spread of the matrix at the top left end of the graph between i and j of the image. This showed a change in the activity of tea leaf cells at 100% water content and 27.22%. The most striking change was shown by the differences in the menu bar

classification. Fresh tea leaves showed a menu bar read from 0-50000 colour pixels, whereas tea with a 27.22% menu bar showed a 0-5000 colour pixel figure. This condition indicated that 100% water leaf tea had higher cell biological activity than the biological cell activity at a lower level of water content.

The measurement of the correlation of speckle patterns, proposed by Xu et al., was the time correlation of the historical stain pattern.[5] Memory phenomena were tested using only the M pixels analyzed by THSP.

$$C_{il} = \frac{\sum_{m=1}^{M} THSP(m,i)THSP(m,i+l)}{\sqrt{\sum_{m=1}^{M} THSP^2(m,i) \sum_{m=1}^{M} THSP^2(m,i+l)}}. \quad (3)$$

Finally, the correlation value with the lag "l" was calculated as Equation (4),

$$C_l = \frac{1}{N/2} \sum_{i=1}^{N/2} C_{il}, \quad (4)$$

where N represented the number of columns of the THSP matrix.
Memory could also be tested using Pearson's correlations between all the pixels in the next image and could be seen in equations (5),

$$C_{il} = \frac{< (\mathbf{I}_i - \mu_i)(\mathbf{I}_{i+l} - \mu_{i+l}) >}{\sigma_i \sigma_{i+l}}, \quad (5)$$

$$\mu_a = < \mathbf{I}_a > \text{ and } \sigma_a = \sqrt{< (\mathbf{I}_a - \mu_a)^2 >}$$

Where was the spatial average and standard deviations of all pixels in the image were taken in a moment.

The correlation of THSP with water levels was shown in the following picture. This correlation was obtained by comparing pixels within the THSP matrix numbering 240 lines in a DATA datapack formed by the directory image indicated by the IMAGESDIR variable to analyze the correlations between pixels in the time history speckle pattern represented by red dots. The blue dots were correlations using the Pearson Correlation approach. (5)

a.

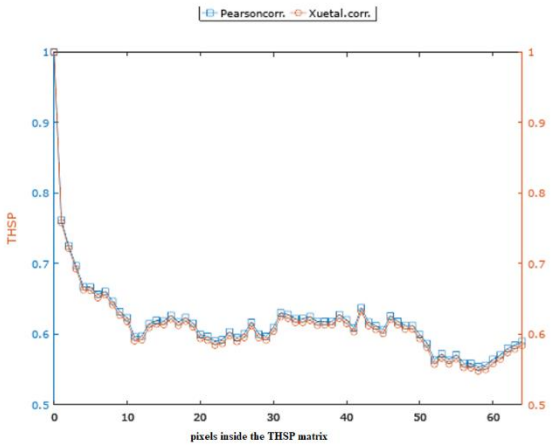


b.

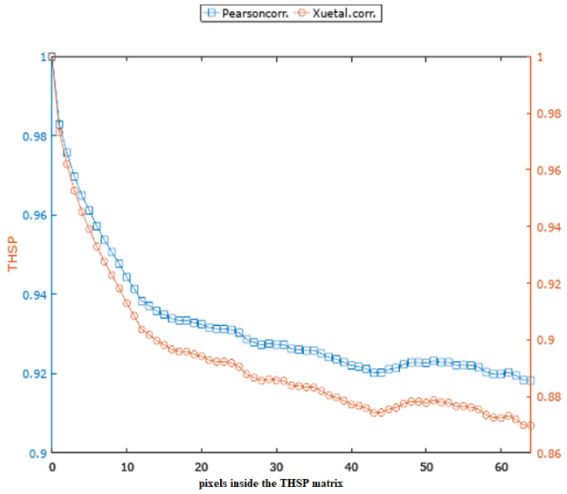


**Figure** 4. THSP matrix correlation with the water content of tea leaves a. 100%; b. 27.72%

Figure 4 showed that at the time of the water content on the tea leaf 100%, there was a correspondence between the THSP pattern and the pattern with Pearson correlation. The possibility of pixel information being repeated every 11 samples was shown in graph a. Whereas at the leaf water level, the 27.72% showed a difference between the THSP pattern and the Pearson correlation pattern, as well as no pattern repetition in the 128 samples taken.

The inertia moment (IM) was based on the construction of the Time History Speckle Pattern (THSP), first proposed by Arizaga[15] In a general way, the calculus of moment inertia is presented in the equation

$$IM = \sum_i \sum_j \frac{COM(i,j)}{Normalization} |i-j|^2 \quad (6),$$

the normalization shown in this equation might be that proposed by Arizaga et al., which made the sum of values in each COM line equal to one, or other normalizations as proposed by[5] to reduce the effect of inhomogeneities in the image analyzed.

$$M_{ij} = \frac{COM(i,j)}{\sum_{lm} COM(l,m)}. \quad (7)$$

The $M_{ij}$ view approach could be seen as a function of the mass probability of the occurrence of a square intensity jump from i to j; thus, the weight factor was $M_{ij} \equiv Pr(i \rightarrow j)$. Thus, the IM value was the expected value of (i−j)2, also known as the first moment of (i− j)2, IM = E[(i− j)2]. Where the IM (IM1) moment submitted by Cardoso and Braga (2016) was 10,

$$E[(i-j)^2] = \sum_{ij} \frac{COM(i,j)}{\sum_{lm} COM(l,m)} (i-j)^2. \quad (8)$$

The calculated IM values from the speckle data were as follows:

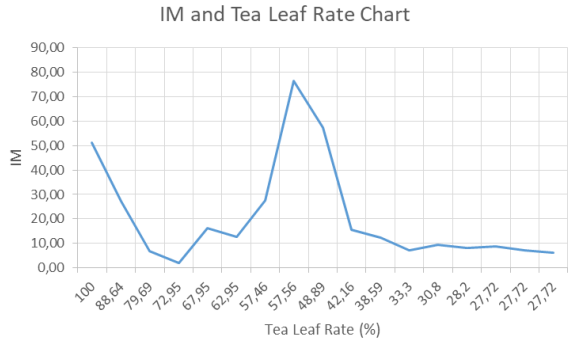


**Figure 5**. Inertia Moment (IM) and Tea Leaf Rate correlation

The data presented showed that the IM value was decreasing at the water level by 100–73%. For water level 73–42%, the peak value IM1 occurred, then the graph consistently descended for water level 43-27%. The IM value was effective in scanning water levels below 57.56% and above 73%.

The Average Value of Difference (AVD) in Equation (10), with IM difference, replaced a square operation with an absolute value, becoming a way to overcome the square effect that increased the perception of high changes on THSP rather than low changes, thus distorting the result CARDOSO; BRAGA, 2014 in[5]

$$AVD = \sum_i \sum_j \frac{COM(i,j)}{Normalization} |i-j| \quad (9)$$

The Absolute Value of the Differences (AVD) method was a modification of the Inertia Moment (IM) performed by modifying the absolute difference between the intensity value of $I_k$ = i in time k and the intensities of $I_{k+1}$ = j in time k + 1 for each value of k. Thus, the AVD method (Equation 11) presented a measurement relative to absolute intensity jump values between sequential images, $I_k$ and $I_{k+1}$.

$$AVD = \sum_{ij} M_{ij} |i-j|. \quad (10)$$

The last equation indicated that the AVD value was the weighed value of |i−j|, where in the Mij weighing factor was calculated from the COM co-occurrence matrix. The AVD was the expected value of |i− j |, also known as the first moment of |I−j|, AVD = E[ |i–j |]. The equation AVD2 determined by the equation, AVD, was the second moment value of AVD with the normalized co-occurrence matrix proposed by[5], becoming AVD = E[ |i-j |2]. This was similar to the inertia moment technique[16] with Cardoso normalization. The results of the AVD analysis were presented in the following figure.

The results of the AVD analysis were presented in the following figure.

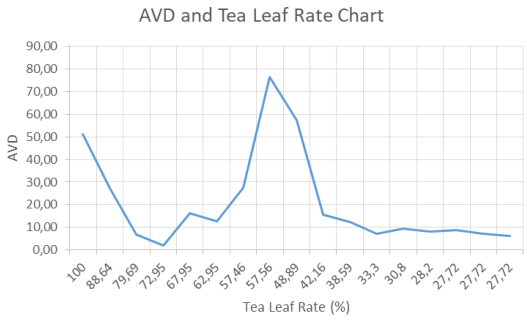


**Figure 6.** Average value of Differences (AVD) and Tea Leaf Rate Correlation

Figure 6 showed that the values of AVD showed an almost identical pattern, indicating a peak at a particular point. Blooded patterns were shown that had a pattern corresponding to the decrease in the water level value of the AVD value. AVD values showed a consistent decrease in water level of upper than 72% and bottom 57.56%. AVD values represented the first moment of the probability mass function Pr(|i−j | = z). AVD was the AVD moment value with the normalized co-occurrence matrix proposed by Cardoso; Braga,[5] becoming AVD = E[ |i−j |2]. This was similar to the inertia moment technique[15] with Cardoso normalization.

## Conclusion

Numerical analysis of THSP, COM, correlation measurements, IM, and AVD could be used to analyze tea leaf speckle images that showed changes in the biological activity of tea leaves. High biological activity occurred at high levels of water content, and decreased biological activity corresponded to a decrease in the water level in the tea leaves.

## Acknowledgment

We would like to acknowledge the LP2M Universitas Islam Negeri Maulana Malik Ibrahim Malang for funding support with the 23-PK-035 number code.

## References

1. Choi B, Kang NM, Nelson JS. Laser speckle imaging for monitoring blood flow dynamics in the in vivo rodent dorsal skin fold model. Microvasc Res. 2004;68(2):143–6.
2. Shao C, Zhang C, Lv Z, Shen C. Pre- and post-harvest exposure to stress influence quality-related metabolites in fresh tea leaves (Camellia sinensis). Sci Hortic. 2021;281:109984.
3. Prawira-Atmaja MI, Maulana H, Shabri S, Riski GP, Fauziah A, Harianto S, et al. Evaluasi kesesuaian mutu produk teh dengan persyaratan standar nasional Indonesia. Jurnal Standardisasi. 2021;23(1):43.
4. Handaratri A, Hudha MI. Pengaruh Metode Pemanasan Dan Penambahan Daun Mint Pada Uji Organoleptik Dan Antioksidan Teh Daun Murbei. Jurnal Penelitian dan Karya Ilmiah Lembaga Penelitian Universitas Trisakti. 2022;173–81.
5. Braga RAJr, Rivera FP, Moreira J. A Practical Guide to Biospeckle Laser Analysis. Theory and Software. 2016. 160 p.
6. Sang X, Cao R, Niu L, Chen B, Li D, Li Q. Lightweight denoising speckle contrast image GAN for real-time denoising of laser speckle imaging of blood flow. Biomed Opt Express. 2025;16(3):1118–42.
7. Dimanche A. Laser speckle contrast imaging as a tool for surgical guidance in neurosurgery. 2024.
8. Konovalov A, Grebenev F, Stavtsev D, Kozlov I, Gadjiagaev V, Piavchenko G, et al. Real-time laser speckle contrast imaging for intraoperative neurovascular blood flow assessment: animal experimental study. Sci Rep. 2024;14(1):1735.
9. Cho KA, Rege A, Jing Y, Chaurasia A, Guruprasad A, Arthur E, et al. Portable, non-invasive video imaging of retinal blood flow dynamics. Sci Rep. 2020;10(1):20236.
10. Pieczywek PM, Nosalewicz A, Zdunek A. A novel application of laser speckle imaging technique for prediction of hypoxic stress of apples. Plant Methods. 2024;20(1):147.

11. Yang S, Li C, Li X, Jiang J, Zhao Y, Wang X, et al. Early detection of fungal infection in citrus using biospeckle imaging. Comput Electron Agric. 2024;225:109293.
12. Linkous C, Pagan AD, Shope C, Andrews L, Snyder A, Ye T, et al. Applications of laser speckle contrast imaging technology in dermatology. JID Innov. 2023;3(5):100187.
13. Duan D, Ma F, Zhao L, Yin Y, Zheng Y, Xu X, et al. Variation law and prediction model to determine the moisture content in tea during hot air drying. Journal of Food Process Engineering. 2022;45(2):e13966.
14. Xu Z, Joenathan C, Khorana BM. Temporal and spatial properties of the time-varying speckles of botanical specimens. Optical engineering. 1995;34(5):1487–502.
15. Arizaga R. Methods of dynamic speckle analysis: statistical analysis. In: Dynamic laser speckle and applications. CRC Press; 2018. p. 95–113.
16. Arizaga R, Trivi M, Rabal H. Speckle time evolution characterization by the co-occurrence matrix analysis. Optics & Laser Technology. 1999;31(2):163–9.